

Cooperative Unfolding of Compact Conformations of the Intrinsically Disordered Protein Osteopontin

Dennis Kurzbach, Gerald Platzer, Thomas C. Schwarz, Morkos Henen, Robert Konrat, Dariush Hinderberger

Correspondence to DH dariush.hinderberger@mpip-mainz.mpg.de or RK: robert.konrat@univie.ac.at

Supporting Information

Contents:

1. Supplementary DEER Spectroscopy
2. Details on time domain calculations
3. Measurements on OPN Single Mutants

1. Supplementary DEER Spectroscopy

In Figure S1c Δ_{eff} is plotted for time traces calculated from $P(R)$ s of random coils of different length as the function of the root-mean-square end-to-end distance, $\langle R^2 \rangle^{1/2}$.¹ This essentially quantifies how an elongation of an interspin distance distribution translates into Δ_{eff} for very broad distance distributions. $P(R)$ for random coils is a Gaussian distance distribution and can be calculated as stated in eq. S1-S3. Note that this is true not only for random coils, but for every distribution that is symmetric around $\langle R^2 \rangle^{1/2}$. The functions of Δ_{eff} were calculated for our specific experimental setup with $\lambda = 0.516$. From Figure S1c one can deduce that Δ_{eff} decays exponentially with $\langle R^2 \rangle^{1/2}$ of random coils if Δ_{eff} is always sufficiently smaller than λ . This is true in our experiments, since $\Delta_{\text{eff}} < 0.45$ in all cases.

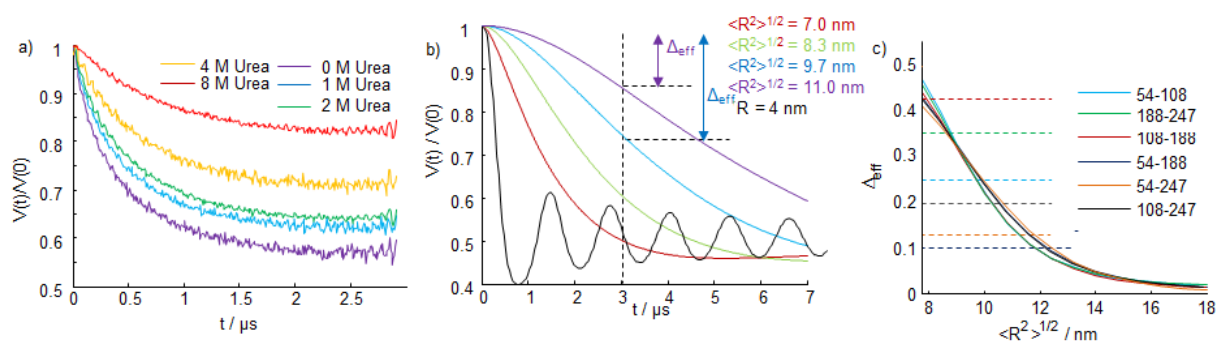


Figure S1. a) DEER time traces of C108-C188 at different urea concentrations. b) Calculated DEER time traces for different interspin distributions distances based on random coils with different $\langle R^2 \rangle^{1/2}$. Δ_{eff} is defined as the signal decay at $t = 3 \mu\text{s}$, as indicated by the double-headed arrows. The black time trace corresponds to a single interspin distance of 4 nm. c) Δ_{eff} as a function of $\langle R^2 \rangle^{1/2}$ of hypothetical random coil polypeptides (distance distribution) with segment numbers corresponding to the residues between the labels of the different double mutants, n. n = 193 (54-247), 80 (108-188), 134 (45-188), 59 (188-247), 54 (54-108) and 139 (108-247). This maps how a certain mean distance translates into a Δ_{eff} -value but has no relevance for real random coils. The dashed lines indicate the maximum observed Δ_{eff} for a given double mutant. Corresponding time traces are similar to those shown in a). Note that

the shift of $\langle R^2 \rangle^{1/2}$ at a given segment number was calculated as changes in Flory's characteristic ratio, c_∞ .

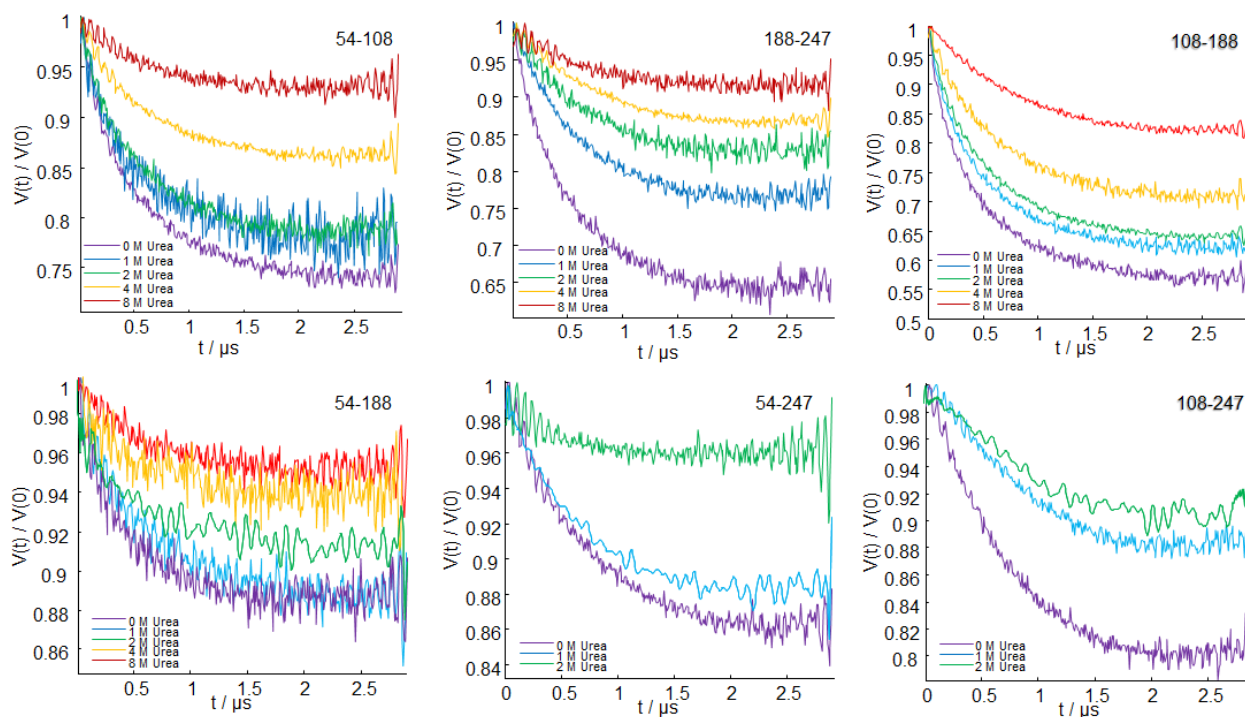


Figure S2. DEER time domain data for all double mutants for different urea concentrations.

Absence of time traces indicates that we observed $\Delta_{\text{eff}} = 0$. Note the different scales of the $V(t)/V(0)$ axes.

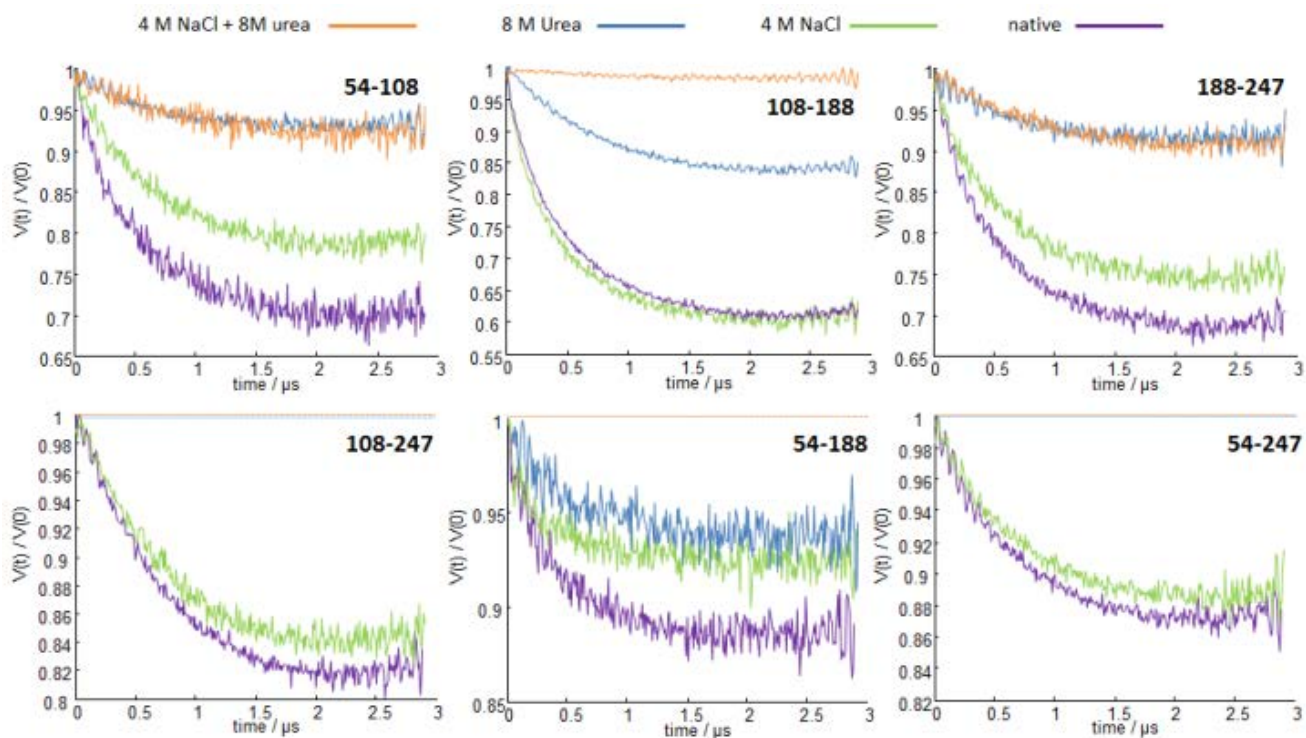


Figure S3. DEER time domain data for all double mutants for different denaturation conditions. Absence of time traces indicates that we observed $\Delta_{\text{eff}} = 0$. Note the different scales of the $V(t)/V(0)$ axes.

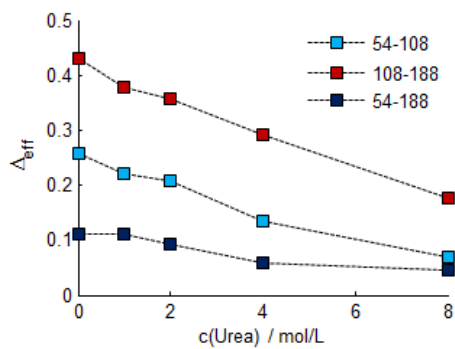


Figure S4. Δ_{eff} for several double mutants as a function of urea concentration.

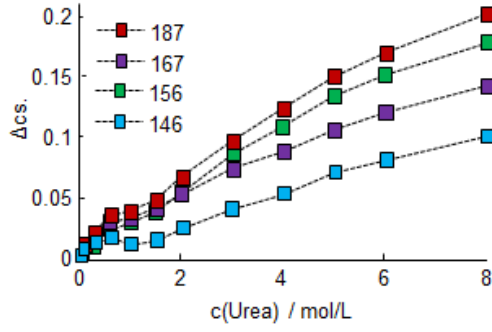


Figure S5. NMR chemical shift changes of selected residues as a function of urea concentration. Note that residue 146 shows a rather different behavior than the other three residues. However, like residue 146 also residues 156 and 167 are located in the central, more compact region of OPN.¹ Only 187 is located in a more flexible section of the IDP.

2. Details on time domain calculations (Figure S1b and c): All calculations were based on random coil models with:¹

$$\langle R^2 \rangle = c_{\infty} n l^2 \quad (\square 1)$$

and

$$P(R, n, l) = \left(\frac{3}{2\pi n l^2} \right)^{3/2} \exp\left(-\frac{3(r - R)^2}{n l^2} \right) \quad (\square 2)$$

Where $P(R, n, l)$ denotes the distribution of end-to-end vectors (see Figure S6a). n is the number of segments and l the segment length. The latter we assumed as the length of one amino acid, which is approximately 0.3 nm. DEER time traces were calculated as:¹⁸

$$V(t) = \sum_R P(\omega_R) V_R(t) \quad (\square 3)$$

with

$$V_R(t) = 1 - \int_0^{\pi/2} \lambda (1 - \cos(\omega_R t)) \sin \theta d\theta \quad (\square 4)$$

θ is the angle between the external magnetic field and the vector connecting observer and pump spins. $P(\omega_R)$ is a distribution of dipolar coupling frequencies, ω_R , that corresponds to $P(R, n, l)$ as:

$$\omega_R = \frac{\mu_0 g_1 g_2 \mu_B}{4\pi \hbar R^3} (3 \cos^2 \theta - 1) \quad (\square 5)$$

g_1 and g_2 denote the g-values of observer and pump spins. These were assumed to be equal. All other constants have their usual meanings. The contribution of compact conformations to $V(3 \mu s) = 1 - \Delta_{eff}$ in dependence of $\langle R^2 \rangle$ can be estimated when calculating:

$$1 - \sum_{R_{min}}^{R_{max}} P(\omega_R) V_R(t) \Big/ 1 - \sum_{R_{min}}^{R(x)} P(\omega_R) V_R(t) \quad (\square 6)$$

Where x denotes a hypothetical fraction of compact conformations of the overall conformational ensemble. Therefore, $R(x)$ has to fulfill $x = \int_{R_{min}}^{R(x)} P(R, n, l) dr / \int_{R_{min}}^{R_{max}} P(R, n, l) dr$ (see Figure S6a). R_{min} is depending on the pump pulse length, τ_p , of a DEER experiment. For $\tau_p = 12$ ns $R_{min} = 1.6$ nm.² R_{max} is approximately 40 nm as calculated by Jeschke and co-workers.³ For $x = 0.05$, that is the cooperatively folded states are estimated to the most compact 5 % of $P(R, n, l)$ and for $t = 3 \mu s$ eq. S6 yields the function plotted in Figure S6b.

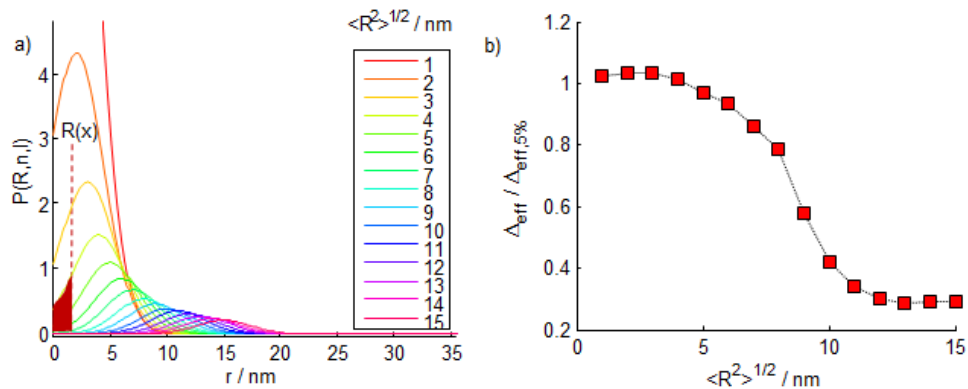


Figure S6. a) End-to-end vector distributions of random coils for different $\langle R^2 \rangle$. $R(x)$ is defined as the distance at which the integral between R_{min} and $R(x)$ matches $x\%$ of the total integral of $P(R, n, l)$. c_{∞} was assumed as 2. b) Inverse contribution of the most compact 5% of conformations of the distributions in a) to Δ_{eff} . A value of 0 means that the DEER signal is totally dominated by the most compact 5% of the conformational ensemble. Values below approximately $\langle R^2 \rangle^{1/2} = 5$ nm cannot be interpreted reliably, since most distances are below 1.6 nm, which is the lower sensitivity limit of the performed DEER measurements. Very long distances are subject to uncertainties, too, since the decay of the DEER signal becomes very shallow. Note that negative distances were treated by their absolute values in $P(R)$.

Judging from Figure S6, one can state that with increasing $\langle R^2 \rangle$ the contribution of compact conformations to Δ_{eff} increases. Yet, we only use this as a qualitative argument, since all the calculations are performed for random coil models and the most compact 5% of conformations are assumed as the cooperatively folded fraction. For actual OPN however $P(\omega_R)$ does not correspond to a random coil and x remains undetermined.

3. Measurements on OPN Single Mutants

To rule out dimerization of OPN and to gain information on the DEER background functions we performed DEER on the four single mutants C54, C108, C188 and C247. In Figure S7 uncorrected DEER data for C188 at 0.8 mM is shown. These data is representative also for

C54, C108 and C247 and for combinations of all four mutants. In all cases we observed exponential decay functions that can be fitted with eq. 1 that is based on a homogeneous 3D distributions of spins as depicted in Figure S7.

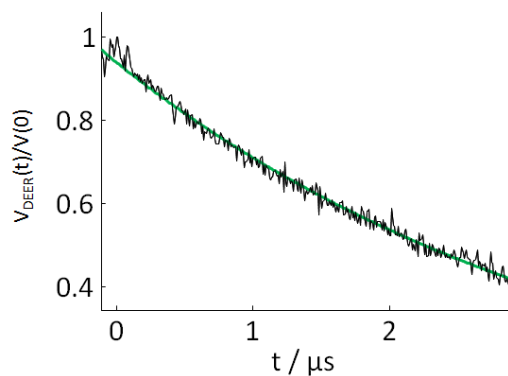


Figure S7. Normalized, raw DEER time domain data for a 0.8 mM solution of single mutant C188 (representative also for C54, C108 and C247; these single mutant data were used for experimental background correction). The green fit corresponds to a homogeneous ($d = 3$) distribution of spins in the freeze-quenched solution (exponential decay). Hence, dimerization of OPN can be ruled out. The green line represents a fit based on a homogeneous exponential decay function.

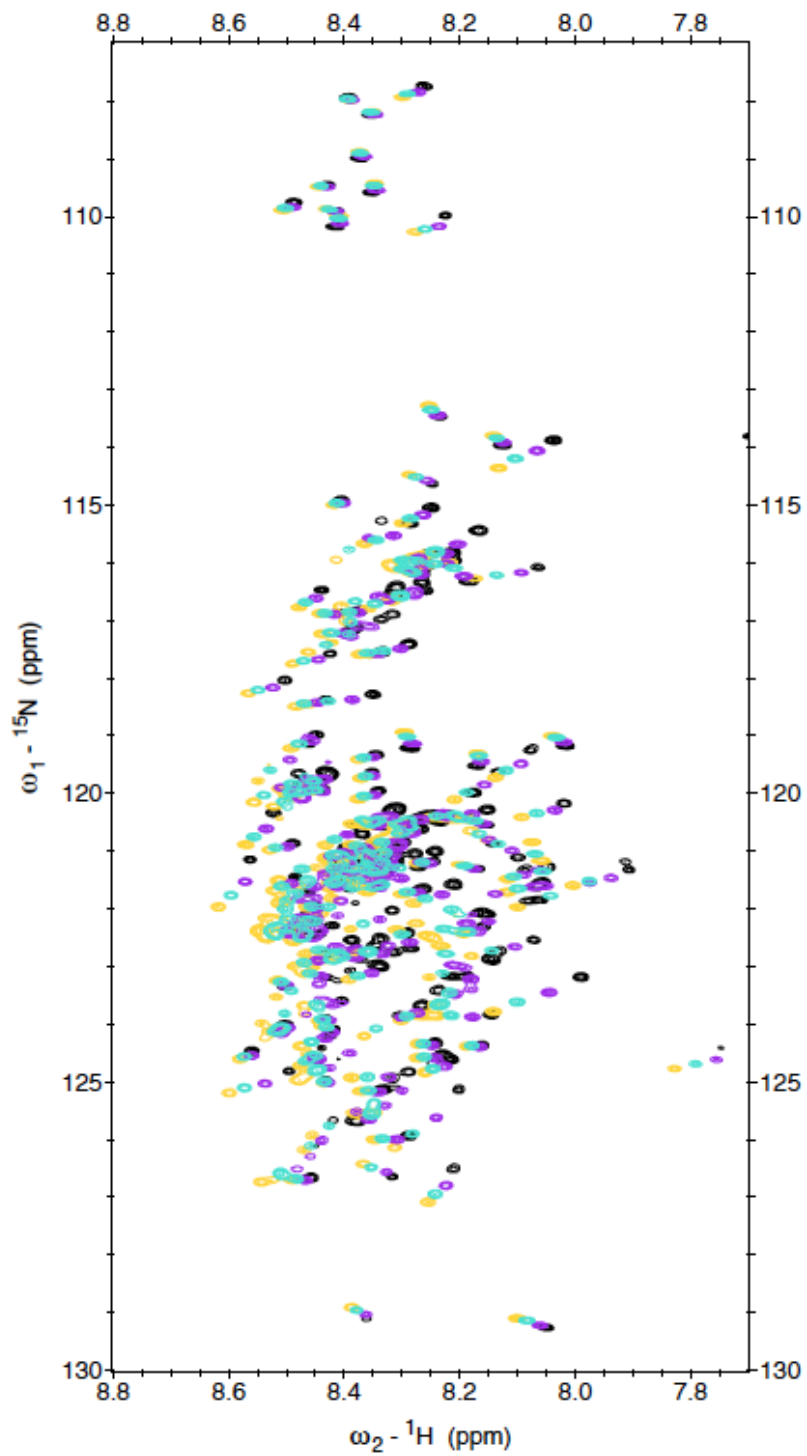


Figure S8. Full ${}^{15}\text{N}$ - ${}^1\text{H}$ HSQC spectra at different urea concentrations. Green: 0 M urea; pink: 2 M urea; blue: 4 M urea; black: 6 M urea

References

- (1) Rubinstein, M.; Colby, R. *Polymer Physics*; Oxford University Press: New York, 2004.
- (2) Tsvetkov, Y. D.; Milov, A. D.; Maryasov, A. G. Pulsed electron-electron double resonance (PELDOR) as EPR spectroscopy in nanometre range; *Russ. Chem. Rev.* **2008**, *77*, 487-520.
- (3) Jeschke, G.; Koch, A.; Jonas, U.; Godt, A. Direct conversion of EPR dipolar time evolution data to distance distributions; *J Magn Reson* **2002**, *155*, 72-82.